Proton and Pion Production Relative to the Reaction Plane in $Au + Au$ Collisions at 10.8 GeV

J. Barrette[4], R. Bellwied[8], S. Bennett[8], P. Braun-Munzinger[6], W. C. Chang[6], W. E. Cleland[5], M. Clemen[5], J. Cole[3], T. M. Cormier[8], G. David[1], J. Dee[6], O. Dietzsch[7], M. Drigert[3], J. R. Hall[8], T. K. Hemmick[6], N. Herrmann[2], B. Hong[6], Y. Kwon[6], R. Lacasse[4], A. Lukaszew[8], Q. Li[8], T. W. Ludlam[1], S. K. Mark[4], R. Matheus[8], S. McCorkle[1], J. T. Murgatroyd[8], E. O'Brien[1], S. Panitkin[6], T. Piazza[6], C. Pruneau[8], M. N. Rao[6], M. Rosati[4], N. C. daSilva[7], S. Sedykh[6], U. Sonnadara[5], J. Stachel[6], E. M. Takagui[7], S. Voloshin[5*], G. Wang[4], J. P. Wessels[6], C. L. Woody[1], N. Xu[6], Y. Zhang[6], C. Zou[6]

(E877 Collaboration)

[1] *Brookhaven National Laboratory, Upton, NY 11973*

[2] *Gesellschaft für Schwerionenforschung, Darmstadt, Germany*

[3] *Idaho National Engineering Laboratory, Idaho Falls, ID 83402*

[4] *McGill University, Montreal, Canada*

[5] *University of Pittsburgh, Pittsburgh, PA 15260*

[6] *SUNY, Stony Brook, NY 11794*

[7] *University of São Paulo, Brazil*

[8] *Wayne State University, Detroit, MI 48202*

(December 11, 1996)

The results of an analysis of proton and charged pion azimuthal distributions measured with respect to the reaction plane in $Au + Au$ collisions at 10.8 GeV/c are presented. Azimuthal anisotropy is studied as a function of particle rapidity and transverse momentum for different centralities of the collisions. The triple differential (in rapidity, transverse momentum, and azimuthal angle) distributions are reconstructed. The comparison of the results with the previous analysis of charged particle and transverse energy flow as

---

*On leave from Moscow Engineering Physics Institute, Moscow, 115409, Russia

well as with model predictions are presented.

I. INTRODUCTION

Collective phenomena play an important role in heavy ion collisions, but for a long time it was considered that at the collision energies much greater than 1 GeV/nucleon only longitudinal and azimuthally symmetric transverse radial flow survive. During the last few years the situation has changed drastically. Anisotropic, directed as well as elliptic, flow has been observed at the BNL AGS [1,2], and there appeared a strong indication of elliptic flow at the CERN SPS [3]. The theoretical understanding of the effect and model calculations involving anisotropic flow have progressed a lot; different anisotropic flow patterns have been linked to such phenomena, as quark-gluon plasma production and softening of the equation of state [4–6], and mean-field formation during the fireball evolution [7,8]. Anisotropic flow become an essential part of the global picture of heavy ion collision at ultrarelativistic energies [9]. The appropriate tools for flow study at high energies have been developed [10,11]. It was also noticed that anisotropic flow could be important for other measurements, such as quantum interferometry [12,13].

In the current paper we present the results of the analysis of anisotropic transverse collective flow of identified particles, namely protons and charged pions, detected by the E877 spectrometer in $Au+Au$ collisions at 10.8 GeV/c. The data were taken during the 1993 Fall run. Using our calorimeter data we explicitly reconstruct the reaction plane event-by-event, and analyze the particle production with respect to this plane. A similar analysis of charged multiplicity and transverse energy flow was performed in [2]. There, a strong directed flow has been observed, as well as elliptic flow with the main axis in the reaction plane, opposite to the "squeeze-out" effect at lower energies. Here, we apply the same procedure to determine the triple differential distributions $d^3N/(dp'_x dp'_y dy)$ of identified protons and charged pions, using the E877 spectrometer data. By prime we denote the quantities in the coordinate system defined by the reaction plane; for example, the azimuthal angle in this system we denote as $\phi' = \phi - \Psi_r$, where Ψ_r is the reaction plane angle in the fixed laboratory frame.

The paper is organized as following. After the description of the apparatus we discuss the whole procedure of the analysis. In the following sections we present first the results of the Fourier analysis of particle azimuthal distributions in different rapidity bins and for different centralities of the collision. These results are to a large extent independent from the uncertainties in the spectrometer efficiency and the detector acceptance. Then the results on triple differential multiplicities and related quantities (such as mean projection of the transverse momentum onto the reaction plane $\langle p_x \rangle$, and effective slope parameters) are discussed. Different flow scenarios are discussed from the point of view of the observed dependence of the flow signal on the particle transverse momentum p_t. We compare our measurements with the estimates of nucleon and pion flow derived from the measurements of charged particle and transverse energy flow [2], as well as with model (RQMD [14] and ARC [15,16]) predictions. Finally we summarize our results.

II. APPARATUS

The E877 apparatus is shown in Fig. 1 and is described in detail elsewhere [2,17]. In the E877 setup, charged particles, emitted in the forward direction, and passed through the collimator ($-134 < \theta_{horizontal} < 16$ mrad, $-11 < \theta_{vertical} < 11$ mrad), are analyzed by the high resolution magnetic spectrometer. The spectrometer identifies particles via simultaneous measurements of momentum and velocity. The momentum of each particle is measured using two drift chambers (DC2 and DC3, position resolution about 300 μm) whose pattern recognition is aided by four Multi-Wire Proportional Chambers (MWPC). The average momentum resolution is $\Delta p/p \approx 4\%$. Time-of-Flight hodoscope (TOFU) located behind the tracking chambers provides the time-of-flight with typical resolution of 85 ps. Spectrometer acceptance covers mostly projectile fragmentation region. More on acceptance for different particle species can be found in [17].

Flow of different particles might be very different in both magnitude and sign. A small admixture in the particle sample of other particle species could heavily bias the final results. Due to this reason, in the current analysis strict requirements are applied for particle identification. Using *momentum vs mass*^{2} plot we select hits in the region of $1.5\,\sigma$ around m^2 peak and reject everything what belongs to $3\,\sigma$ region of other particles.

The centrality of the collision and the determination of the reaction plane orientation are made using the transverse energy measured by the Target Calorimeter (TCal), and Participant Calorimeter (PCal). Both of them have 2π azimuthal coverage, and, combined together, they have nearly complete polar coverage as viewed from the nucleon-nucleon center of mass: TCal and PCal cover the pseudorapidity regions $-0.5 < \eta < 0.8$ and $0.8 < \eta < 4.2$, respectively.

III. ANALYSIS

The structure of the analysis is very similar to the one used in [2], and many details can be found there. The azimuthal anisotropy of particle production is studied by means of Fourier analysis [1,2,11]. Namely we study the rapidity, transverse momentum, and centrality dependence of Fourier coefficients v_n (amplitude of n-th harmonic) in the decomposition:

$$E\frac{d^3N}{d^3p} = \frac{d^3N}{p_t dp_t dy d\phi'} = \frac{1}{2\pi}\frac{d^2N}{p_t dp_t dy}(1 + 2v_1\cos(\phi') + 2v_2\cos(2\phi') + 2v_3\cos(3\phi') + ...). \quad (1)$$

In each event the reaction plane angle is determined by the direction of transverse energy flow in TCal and PCal, and the coordinate system is rotated to make the reaction plane to be the new $x-z$ plane. Note that the coverage of the calorimeters, used for the reaction plane determination, does not overlap with the spectrometer coverage, and thus the analysis is free from the problems related to autocorrelations. The p_x and p_y of identified particles in each event are mapped into the new coordinate system, and the particle distributions are determined with respect to the reaction plane. We have full 2π acceptance only for a very limited p_t range (approximately $p_t \leq 50$ MeV), but the triple differential multiplicity is constructed in full, taking into account 2π range of the reaction plane angle distribution.

Similarly to the analysis [2], the reaction plane angle is determined in four independent pseudo-rapidity windows. The reaction plane resolution is evaluated by studying the correlation between flow angles determined in different windows. Finally, the flow signals are corrected for this resolution. Details of this procedure are described in [2]. In short, the true value of v_n are evaluated by:

$$v_n = v_n^{observed}/\langle\cos(n(\Psi_1 - \Psi_r)\rangle, \quad (2)$$

where $v_n^{observed}$ is the observed signal, and $\langle\cos(n(\Psi_1 - \Psi_r)\rangle$, which characterizes the reaction plane resolution, is the mean cosine of the difference of the reconstructed and true reaction plane angles. The values of $\langle\cos(n(\Psi_1 - \Psi_r)\rangle$ are evaluated using the correlation of flow angles reconstructed in different pseudorapidity regions [2].

The E877 spectrometer has a relatively small azimuthal coverage. Due to this, the analysis of azimuthal anisotropies is rather sensitive to the biases of different kinds, which could simulate event anisotropy and propagate to the final results. So, during the off-line analysis it was found that a small fraction of the recorded events ($\leq 2\%$), so called "blast" events, have anomalously high number of hits in the drift chambers. Such events were found to correlate with the occupancy of the spectrometer and, consequently, to the orientation of the reaction plane. This bias (of the order of a percent) was avoided by performing the "flattening" (see Appendix) of the reaction plane angle distribution only on the "non-blast" event sample. The efficiency of the spectrometer (typically of the order of 90%) was also found depending on the spectrometer occupancy. A special correction for this effect (contribution to v_1 of the order of $\leq$ 2–3%) was developed and checked by Monte-Carlo simulation of the spectrometer. This correction is based on the weighting of each track in accordance with the local track density in the drift chambers in each event. A special precaution was also taken to get the reaction plane angle distribution as flat as possible (see Appendix A).

The Fourier coefficients of azimuthal distributions evaluated by the procedure described above (corrected for the reaction plane), were combined with the measurements of p_t and rapidity spectra [17]. In this way the triple differential distributions in y, p_t, and ϕ' (see formula (1)) were found and analyzed.

IV. RESULTS

A. Directed Flow

We quantify directed flow by v_1, the amplitude of the first harmonic in Fourier decomposition of azimuthal particle distribution. The coefficient v_1 is analyzed as a function of transverse momentum for different rapidity bins and collision centralities. Four centrality regions, selected in accordance to PCal E_T: $150 < E_T < 200$, $200 < E_T < 230$, $230 < E_T < 270$, and $E_T > 270$ GeV, correspond to the values of $\sigma_{top}/\sigma_{geo} \approx$ 23–13%, 13–9%, 9–4%, and <4%, respectively (see Fig. 4 in [2]).

The results for $v_1(p_t)$, corrected for the reaction plane resolution, are presented in Figures 2–4 for protons and charged pions. Proton production is very strongly correlated with the orientation of the reaction plane. Protons of larger p_t have larger value of v_1 with some tendency to saturation in the highest p_t region. The largest observed value of v_1 is about 0.45, which corresponds to a change in the high p_t proton yield almost in 10 times from $\phi' = \pi$ to $\phi' = 0$ (see also Fig. 8 below). Note that for the lowest centrality region protons with very small transverse momentum have a tendency to flow in the opposite direction. This could be an indication of transverse isotropic expansion and will be studied in details elsewhere [18] using high statistics of 1994 run data.

Both positive and negative pions exhibit small "anti-flow". Note very different behaviour of proton and pion signals as a function of p_t. For protons v_1 grows almost linearly with p_t; for pions v_1 saturates very fast. The average value of $v_1^\pi \approx -0.05 - -0.1$. Positive pions of low p_t seem to have bigger azimuthally anisotropic effect, $v_1^{\pi^+}$ saturates already at $p_t \approx 0.05\ GeV$. The rapidity dependence of directed flow of positive and negative pions is also slightly different. At beam rapidity positive pions exhibit noticeably larger flow signal than negative pions.

Centrality dependence of all flow signals is well pronounced. The magnitude of flow for all particles decreases for more central collisions.

Note that independent of flow scenario $v_1(p_t)$ must vanish at $p_t = 0$, due to continuity of the spectra. This fact can be used for an estimate of a systematic error in the results of the analysis.

B. Higher Harmonics in Azimuthal Distributions

Higher harmonics (v_2 and v_3) have been also analyzed. The accuracy in the evaluation of the contribution of higher harmonics deteriorates with increasing harmonic order due to the limited reaction plane resolution (see the discussion in [2]). This results in larger relative errors. Our results for the proton elliptic flow (amplitude of the second harmonic in the proton azimuthal distributions) as a function of transverse momentum is presented in Fig. 5. Possibly due to the limited p_t acceptance we do not observe significant signal in the rapidity region $y < 2.4$. As for the beam rapidity, clear signal is observed in hight p_t region. Note that the positive value of v_2 corresponds to an elliptic shaped distribution with the major axis lying in the reaction plane. Pions do not exhibit any elliptic flow within out acceptance at the level of a few percent.

Our (absolute) accuracy in measuring of v_3 is about 0.1. For all particles, rapidities and centralities of the collision the signals are consistent with zero within this accuracy.

C. Mean p_x and parameterization of d^3N/d^3p'

Weighted with p_t the coefficient v_1 yields widely used in flow analysis quantity $\langle p_x \rangle$, the mean value of transverse momentum projected onto the reaction plane:

$$\langle p_x \rangle = \frac{1}{N} \int \frac{dN}{dp_t} (v_1 \cdot p_t) dp_t. \tag{3}$$

As any other integral quantity, $\langle p_x \rangle$ is less informative in comparison with v_1, but in order to compare our results with others we calculate this quantity using the spectra [17] measured by the same apparatus. The results for centrality region $200 < E_T < 230\ GeV$ ($\sigma_{top}/\sigma_{geo} \approx$0.009 – 0.013), shown in Fig. 6, cover mostly the forward rapidity region. Due to the limited p_t acceptance the reliable evaluation of this quantity is possible only in rather small region of rapidity. Where it becomes necessary, we extrapolate dN/dp_t to high p_t region using thermal parameterization. The filled points in Fig. 6 correspond to $\langle p_x \rangle$ calculated in accordance to formula (3) and using the parameterization of $v_1(p_t)$ shown in Fig. 2 by upper curves (formulae (11)). Note that due to a small contribution of the low p_t region to $\langle p_x \rangle$ the small difference between the parameterization and the data in this region do not contribute to the final result. The entire contribution of the non-measured part of the spectra to $\langle p_x \rangle$ is relatively small at beam rapidity (less than 10%), where the acceptance is good. At rapidity about $y = 2.6$ this contribution accounts for about 40% of the value of $\langle p_x \rangle$. The error-bars do not include the uncertainty in the effective slope parameters used for the spectra extrapolation.

The same quantity ($\langle p_x \rangle$) can be estimated using different parameterizations of the invariant triple differential distribution, which have $\langle p_x \rangle$ as a parameter. We use two functional forms to parameterize d^3N/d^3p' of protons in each rapidity bin considered. The first one reads:

$$\Phi_1 \sim \frac{dN}{dy} \cdot m'_t \exp\left(-\frac{m'_t - m}{T}\right), \tag{4}$$

$$m'_t = \sqrt{(p'_x - \langle p_x \rangle)^2 + p'^2_y + m^2} \tag{5}$$

With the effective slopes from the spectra [17] we use the function (4) to fit the experimental values of $v_1(p_t)$ (see Fig. 2, lower dashed curves). The extracted values of $\langle p_x \rangle$ are shown in Fig. 6 as open points. The difference between two results obtained with two different parameterization (filled and open point in Fig. 6) could give an idea about the systematic uncertainty.

The possible elliptic shape of the azimuthal distribution was checked by fitting the entire spectra by the function:

$$\Phi_2 \sim \frac{dN}{dy} \cdot \exp\left(-\frac{(p'_x - \langle p_x \rangle)^2}{2\sigma^2_{p_x}} - \frac{p'^2_y}{2\sigma^2_{p_y}}\right) \tag{6}$$

There are three parameters in this function: $\langle p_x \rangle$, σ_{p_x}, and σ_{p_y}. The observed difference between σ_{p_x} and σ_{p_y} (σ_{p_y} is larger than σ_{p_x} at about 10%), agrees with the measurements of the second harmonic.

Anisotropic flow can be also characterized by the inverse slope of p_t spectra of particles emitted at different azimuthal angles. We extract this slope by fitting the spectra in the region $p_t > 0.1\ GeV$ by thermal (Boltzmann) function with the slope parameter T_B depending on the azimuthal angle ϕ':

$$\Phi_3 \sim \frac{dN}{dy} m_t \exp\left(-\frac{m_t - m}{T_B(\phi')}\right). \tag{7}$$

The results of this fit are shown for three rapidity bins in Fig. 7, where T_B is plotted as a function of the azimuthal emission angle, and in Fig. 8, where m_t spectra are shown together with the fit for rapidity interval $2.8 < y < 2.9$. These results are not corrected for the reaction plane resolution. Such a correction would increase the difference between the maximal and minimal values of T_B in about 1.5 times.

V. DISCUSSION

A. Moving thermalized source

One of the simplest pictures of directed flow would be a movement of a thermalized source in the transverse plane. Assuming no radial expansion, the particle invariant spectra from a thermalized source are described by the formula:

$$\frac{1}{m_t}\frac{dN}{dm_t dy d\phi'} \propto E^* e^{-E^*/T}, \tag{8}$$

where T is the temperature, and E^* is the particle energy in the source rest frame. In the case of the source moving along the x axis with velocity β_x (which we call directed flow velocity), the value of E^* can be found by the Lorentz transformation:

$$E^* = \gamma\tilde{E} - p_t\beta_x\gamma\cos(\phi'), \tag{9}$$

where $\gamma = 1/\sqrt{1-\beta_x^2}$, and the energy $\tilde{E}$ is evaluated in the system moving longitudinally with the same velocity as the source, $\tilde{E} = m_t\cosh(y - y^*)$; y^* is the source rapidity. Using (8-9) one finds:

$$v_1 = \frac{I_1(\xi) - (\xi I_0(\xi) - I_1(\xi))T/\tilde{E}}{I_0(\xi) - \xi^2 I_1(\xi)T/\tilde{E}}, \tag{10}$$

where $\xi = p_t\beta_x\gamma/T$, and $I_0(\xi)$ and $I_1(\xi)$ are the modified Bessel functions. For protons $m_t \gg T$ and v_1 does not depend on, in general unknown, value of y^*. Taking into account that expected $\beta_x \ll 1$, for relatively small value of p_t we have almost linear dependence of v_1 on p_t:

$$v_1 \approx \frac{I_1(\xi)}{I_0(\xi)} \quad \left(\approx \frac{p_t\beta_x}{2T}\right). \tag{11}$$

Taking the data on v_1 for protons from Fig. 2 and T_B from [17] as T, for the rapidity region close to the beam rapidity one gets the values of $\beta_x \approx$ 0.04–0.06. In fig. 9, the extracted β_x of the proton source are shown for different proton rapidities and collision centralities.

For pions we observe v_1 with almost now dependence on p_t. It means that the physics of such flow is different from the moving source (just as one could expect). The possible explanation of pion flow signal would be an absorption in nuclear matter. For pions produced somewhere in the center of the collision and moving in the forward direction with the velocity close to the speed of light one would expect more nuclear matter from the direction of flow (positive x' in our system) and, consequently, more absorption. An assumption on independence of the absorption cross section on pion p_t would explain the observed $v_1(p_t)$ behaviour.

B. Comparison with the results on N_{ch} and E_T flow

In the paper [2] under a few simple assumptions transverse energy and charged particle flow was disentangled in nucleon and pion flow. Both were studied as a function of pseudorapidity. Using this results and making a simple parameterization of proton triple differential distributions from [17,20] we estimate $\langle p_x \rangle$ as a function of rapidity. In particular we use:

$$\frac{d^3n}{dyp_tdp_t} \propto \exp(-\frac{(y-y_0)^2}{2\cdot 1.6^2})\cdot m_t\ \exp(-\frac{m_t-m}{T_b(y)}), \tag{12}$$

$$T_b(y) \approx 0.26\exp(-\frac{(y-y_0)^2}{2\cdot 1.06^2})\ GeV. \tag{13}$$

Using this parameterization we calculate mean rapidity (weighted with E_t) as a function of pseudorapidity $y(\eta)$. Then assuming $v_1^{E_t(y)}$ to be close to $v_1^{p_t(\eta)}$, one gets $\langle p_x \rangle$ in the region around mid-rapidity.

$$\langle p_x \rangle(y) \approx \langle p_t \rangle(y)\cdot v_1^{E_t}(\eta) \tag{14}$$

These data are presented in Fig. 10 along with our current analysis results (using the upper parameterizations from Fig. 2; the error in effective temperature of the order of 7% have been added). The horizontal error-bars represent the widths of the rapidity region actually contributing to the pseudorapidity regions used to get v_1 for this particular rapidity.

In the whole the agreement between the results of the current analysis of spectrometer data (covered mostly the projectile fragmentation region) and results derived from measurements of E_T and N_{ch} flow is good. But it should be taken into account that the (systematic) uncertainties just in the rapidity region where two measurements can be compared are rather large.

Taken together, two measurements provide $\langle p_x \rangle$ as a function of rapidity in the entire rapidity range.

C. Comparison with model predictions

We compare our results on $\langle p_x \rangle$ with the predictions of RQMD event generator [14], version 1.08, in Fig. 10. We use the same version of RQMD as was used for comparison of our earlier results on pseudorapidity distributions [19] and E_T and N_{ch} flow [1,2]. On the other hand new versions of RQMD 2.2 and 2.3 have been developed [21]. In spite of the fact that version 2.2 is run in the so-called "cascade" mode and is expected to be close to version 1.08, it is found that it predicts the values of $\langle p_x \rangle$ almost two times smaller. The version 2.3 ("mean field" mode) predicts about 10–20% larger values of $\langle p_x \rangle$ than 1.08 and is more close to our data.

The results of ARC (10% centrality) calculations [16] if overlaid with our data would show a very good agreement. Unfortunately, from the preprint [16] it is not clear whether the authors use an inclusive centrality cut (when all events in the top 10% of centrality are included) or exclusive cut (as was used in our analysis). For more complete comparison it would be also important to compare our spectra with the ones from ARC.

VI. SUMMARY AND CONCLUSION

The measured flow signals of identified particles show that in the mid-central collisions protons (nucleons) exhibit strong directed flow; pions flow in the opposite direction. The results are consistent with nucleon and pion flow derived from the measurement of E_T and N_{ch} flow within complementary acceptance [2]. Taken together they represent the directed flow measurement in the entire rapidity region in Au+Au collisions at 10.8·A GeV/c.

The observed positive values of the second harmonic amplitudes of the proton azimuthal distributions correspond to the preferential particle emission in the reaction plane. This observation agrees with our previous measurements of E_t and N_{ch} elliptic flow [2].

The nearly linear dependence of proton flow signal v_1 on p_t can be interpreted in the picture of a transversely boosted thermal source. The boosting velocity β_x appeared to reach the values of 0.1 in the beam rapidity region and mid-central collision. The negative v_1 and much weaker p_t dependence for pions could be a results of the pion absorption by the spectator nucleons.

ACKNOWLEDGEMENTS

We thank the AGS staff, W. McGahern and Dr. H. Brown for excellent support and acknowledge the untiring efforts of R. Hutter in all technical matters. Financial support from the US DoE, the NSF, the Canadian NSERC, and CNPq Brazil is gratefully acknowledged. One of us (JPW) thanks the A. v. Humboldt Foundation for support, while another (WCC) acknowledges the financial support from Gottlieb Daimler- and Karl Benz Stiftung during his stay in Heidelberg, Germany, where part of this work was done.

APPENDIX

A. Flattening of the Reaction Plane Distribution

Due to the possible wrong gains and dead towers in the calorimeters the reconstructed reaction plane distribution generally is not flat. We apply the following procedures to correct for this non-flatness of the distribution.

Any flattening of the distribution means the correction to the reaction plane angle. We explicitly introduce this correction defining a new angle as:

$$\psi_r' = \psi_r + \Delta\psi_r. \tag{15}$$

where $\Delta\psi_r$ is written in the form:

$$\Delta\psi_r = \sum_n (A_n \cos(n\psi_r) + B_n \sin(n\psi_r)) \tag{16}$$

Requiring the vanishing of the n-th Fourier moment of the new distribution, the coefficients A_n and B_n can be evaluated by the original distribution.

$$B_n = \frac{2}{n}\langle\cos(n\psi_r)\rangle, \tag{17}$$

$$A_n = -\frac{2}{n}\langle\sin(n\psi_r)\rangle, \tag{18}$$

where $\langle\rangle$ means an event average. It gives:

$$\psi_r' = \psi_r + \sum_n \frac{2}{n}(-\langle\sin(n\psi_r)\rangle \cos(n\psi_r) + \langle\cos(n\psi_r)\rangle \sin(n\psi_r)) \tag{19}$$

In practice, we flatten the reaction plane distribution up to the fourth harmonic (n=4). Note that due to the small values of A_n and B_n (typically of the order of a few percent) such a flattening of the distribution does not have any effect on the reaction plane resolution.

FIGURE CAPTIONS

1. The E877 apparatus.

2. The transverse momentum dependence of the first moment (v_1) of proton azimuthal distribution for different particle rapidities and centralities of the collision (PCal E_T, shown in GeV). For the description of dash lines see Section V.

3. The same as Fig. 2 for positive pions.

4. The same as Fig. 2 for negative pions.

5. The transverse momentum dependence of the second moment (v_2) of proton azimuthal distribution for different particle rapidities and centralities of the collision.

6. Mean projection of the proton transverse momentum onto the reaction plane, $\langle p_x \rangle$, as a function of rapidity. Open points (shifted to the left by 0.05 for clarity) correspond to the fit by function (4).

7. The dependence of inverse (Boltzmann) slope (T_B) of proton distribution as a function of azimuthal angle. The open points are the reflection of filled ones around $\phi' = 0$.

8. The fit of proton m_t distributions in the rapidity interval $2.8 < y < 2.9$ by function (7). The effective slope values and centrality (PCal E_t) are shown in GeV. The open (filled) points correspond to $-\pi/4 < \phi' < \pi/4$ ($3\pi/4 < \phi' < 5\pi/4$).

9. Transverse velocity β_x of the thermal (proton) source for different rapidities and centralities of the collision (PCal E_T, in GeV).

10. Mean projection of the proton transverse momentum onto the reaction plane $\langle p_x \rangle$ as a function of rapidity. Open circles, triangles and squares are the reflection of filled ones. The results derived from measurements [2] are shown by stars. The histograms correspond to RQMD 1.08.

[1] E877 Collaboration, J. Barrette *et al.*, Phys. Rev. Lett. **70**, 2996(1993).

[2] E877 Collaboration, J. Barrette *et al.*, preprint nucl-ex/9610006, Phys. Rev. C, in print; T. Hemmick for the E877 Collaboration, Proc. Quark Matter '96, Nucl. Phys. **A610** (1996), in print.

[3] T. Wienold for the NA49 Collaboration, Proc. Quark Matter '96, Nucl. Phys. **A610** (1996), in print.

[4] C.M. Hung and E.V. Shuryak, Phys. Rev. Lett. **75**,4003 (1995).

[5] L. Bravina, L.P. Csernai, P. Lévai, and D. Strottman, Phys. Rev. C **50**, 2161 (1994); L. Bravina, Phys. Lett. B **344**, 49 (1995).

[6] B.A. Li, C.M. Ko, G.Q. Li, Phys. Rev. C **54**, 844 (1996).

[7] B.A. Li, C.M. Ko, Phys. Rev. C **52**, 2037 (1995); **53**, R22 (1996).

[8] H. Sorge, Preprint SUNY-NTG 96-40, nucl-th/9610026, 1996.

[9] J. Stachel, Proc. Quark Matter '96, Nucl. Phys. **A590** (1996), in print.

[10] J. Y. Ollitrault, Phys. Rev. **D46**, 229 (1992); Phys. Rev. **D48** 1132 (1993).

[11] S. Voloshin and Y. Zhang, Z. Phys. C **70**, 665 (1996);

[12] D. Miśkowiec for E877 Collaboration, Proc. Quark Matter '95, Nucl. Phys. **A590**, 473c (1995); Proc. Quark Matter '96, Nucl. Phys. **A590** (1996), in print.

[13] S.A. Voloshin and W.E. Cleland, Phys. Rev. C **53**, 896 (1996); Phys. Rev. C **54**, 3212 (1996).

[14] H. Sorge, A.v. Keitz, R. Mattiello, H. Stöcker, W. Greiner, Phys. Lett. **B243**, 7 (1990).

[15] Y. Pang, T. Schlagel, and S. K. Kahana, Phys. Rev. Lett. **68**, 2743 (1992);

[16] D.E. Kahana, Y. Pnag, E. Shuryak, nucl-th/9604008, 1996.

[17] E877 Collaboration, J. Barrette *et al.*, "Proton and Pion Distributions in Au-Au ...", in prepa-

ration;

R. Lacasse for the E877 Collaboration, Proc. Quark Matter '96, Nucl. Phys. **A610** (1996), in print.

[18] E877 Collaboration, J. Barrette *et al.*, in preparation.

[19] E877 Collaboration, J. Barrette *et al.*, Phys. Rev. C **51**, 3309(1995).

[20] Y. Akiba for the E802 Collaboration, Proc. Quark Matter '96, Nucl. Phys. **A590** (1996), in print.

[21] H. Sorge, Proc. Workshop HIPAGS '96, Wayne State University, 1996, in print.

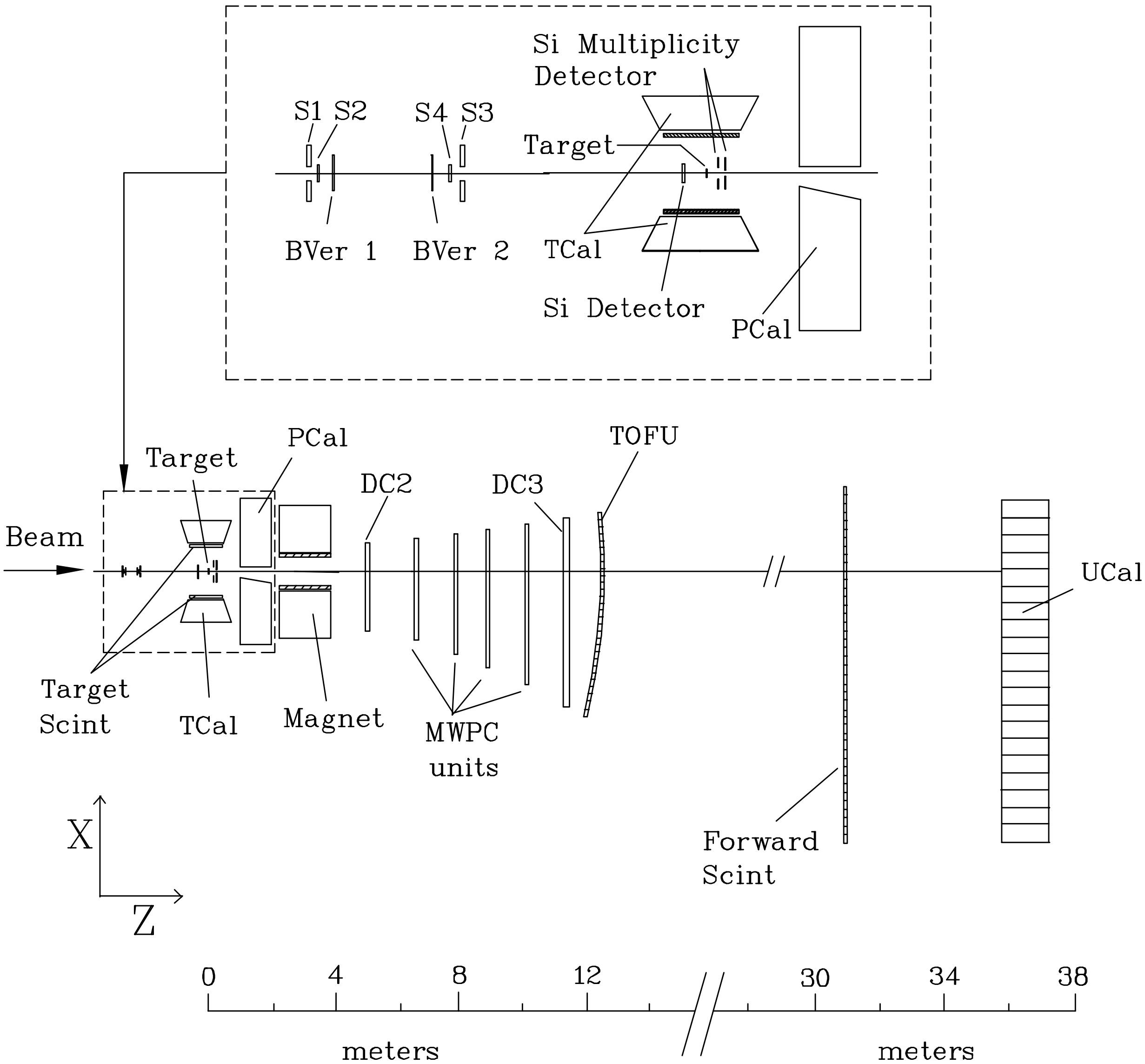

FIG. 1. The E877 apparatus

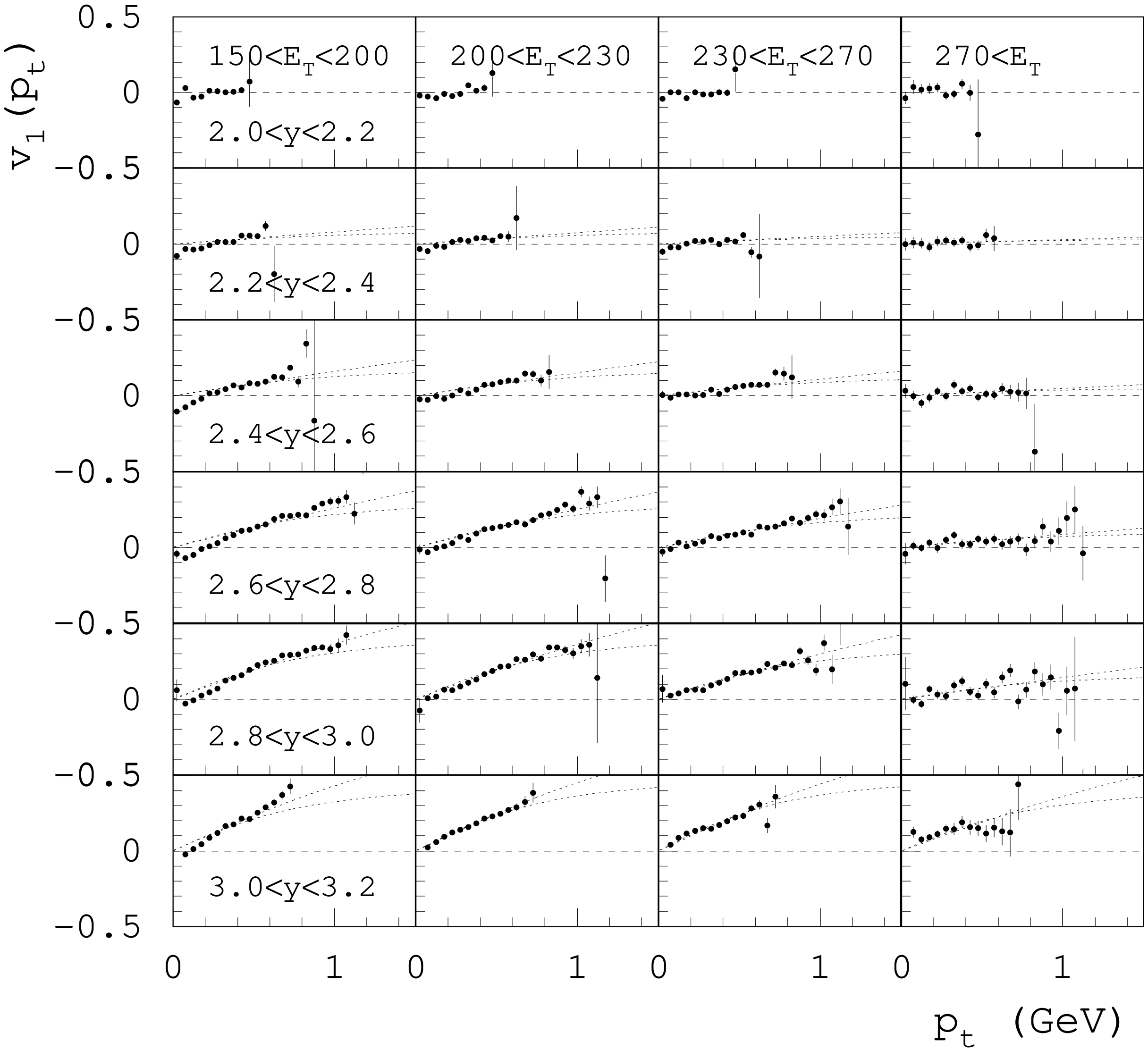

FIG. 2. The transverse momentum dependence of the first moment (v_1) of proton azimuthal distribution for different particle rapidities and centralities of the collision (PCal E_T, shown in GeV). For the description of dash lines see Section V.

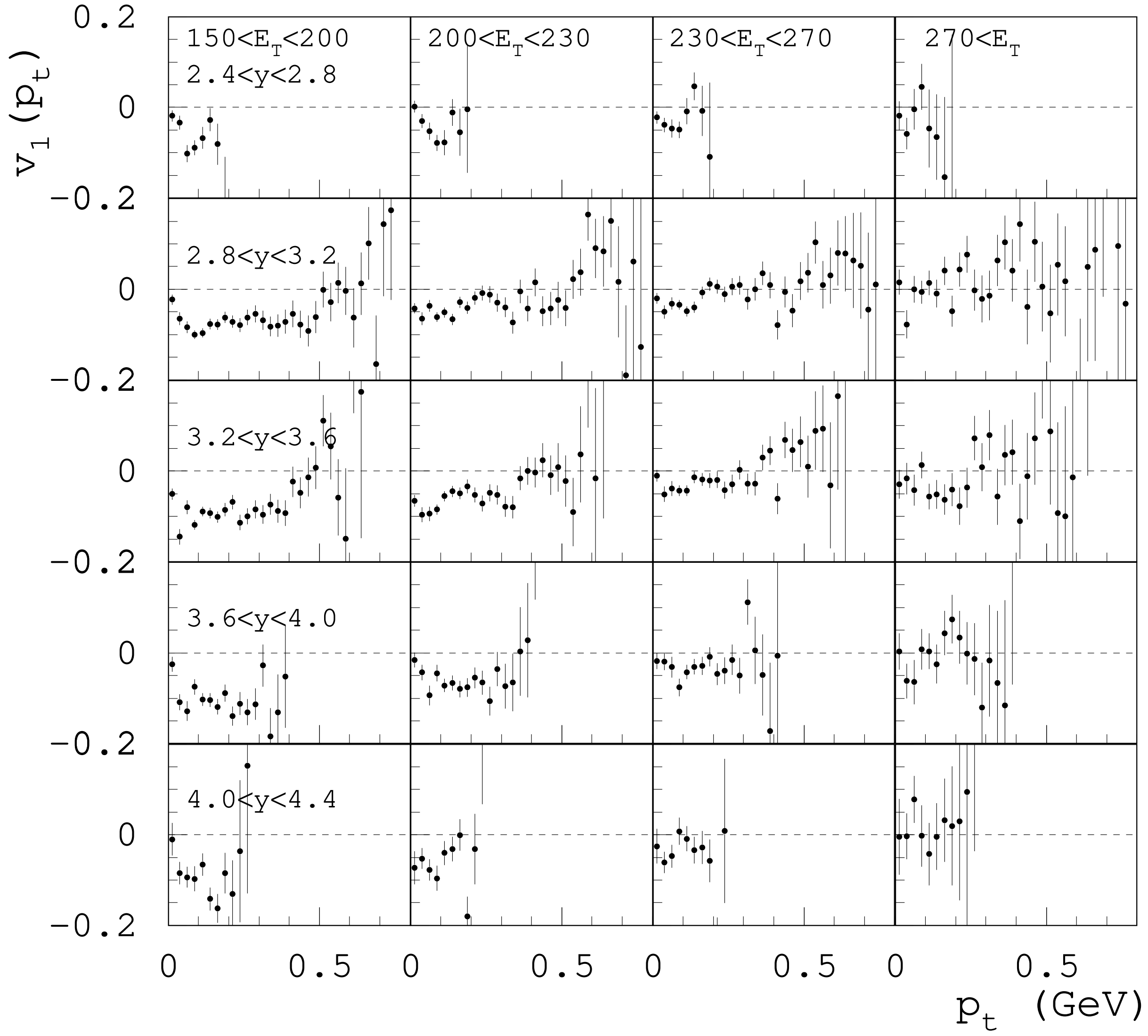

FIG. 3. The same as Fig. 2 for π^+.

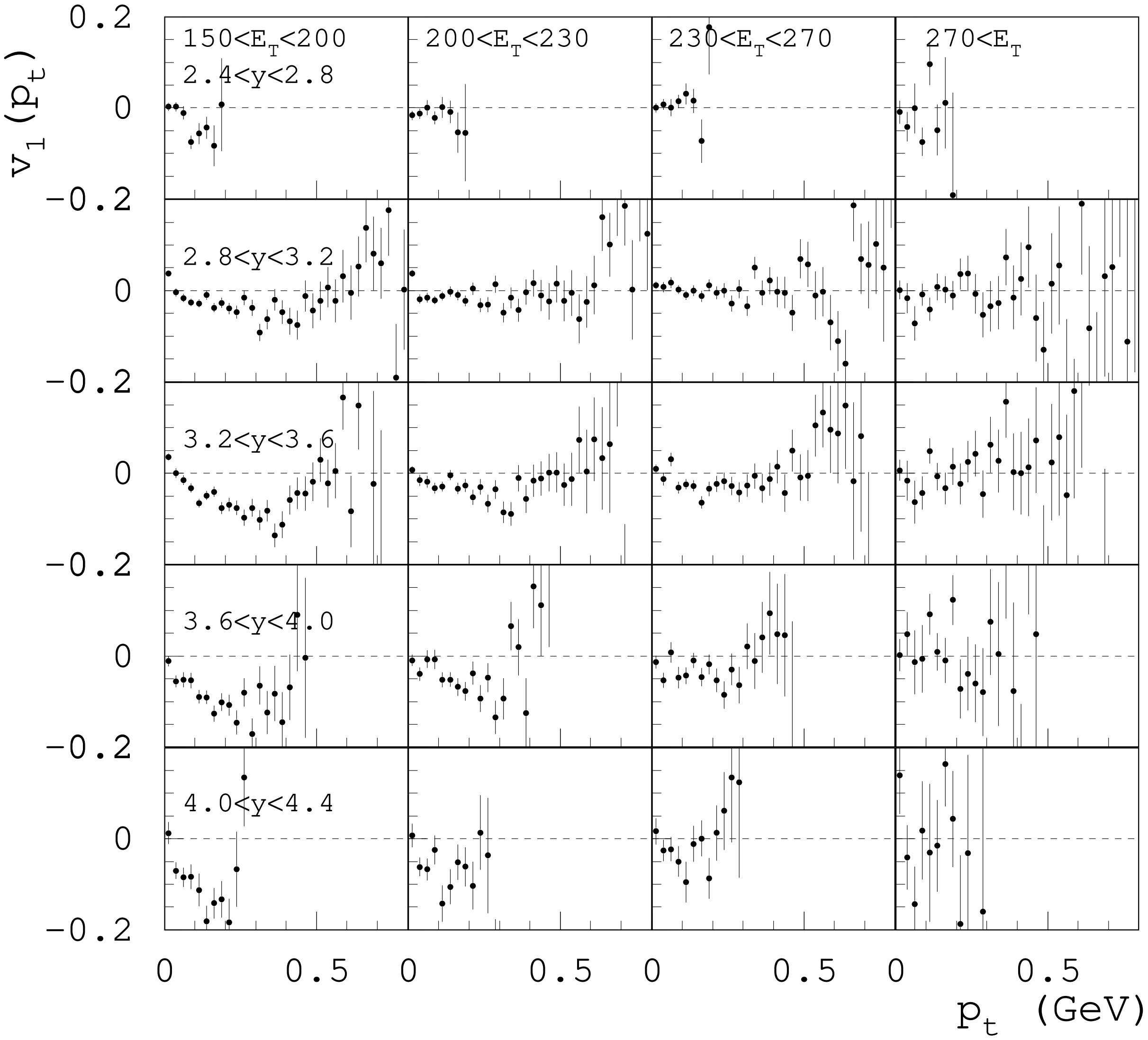

FIG. 4. The same as Fig. 2 for π^-.

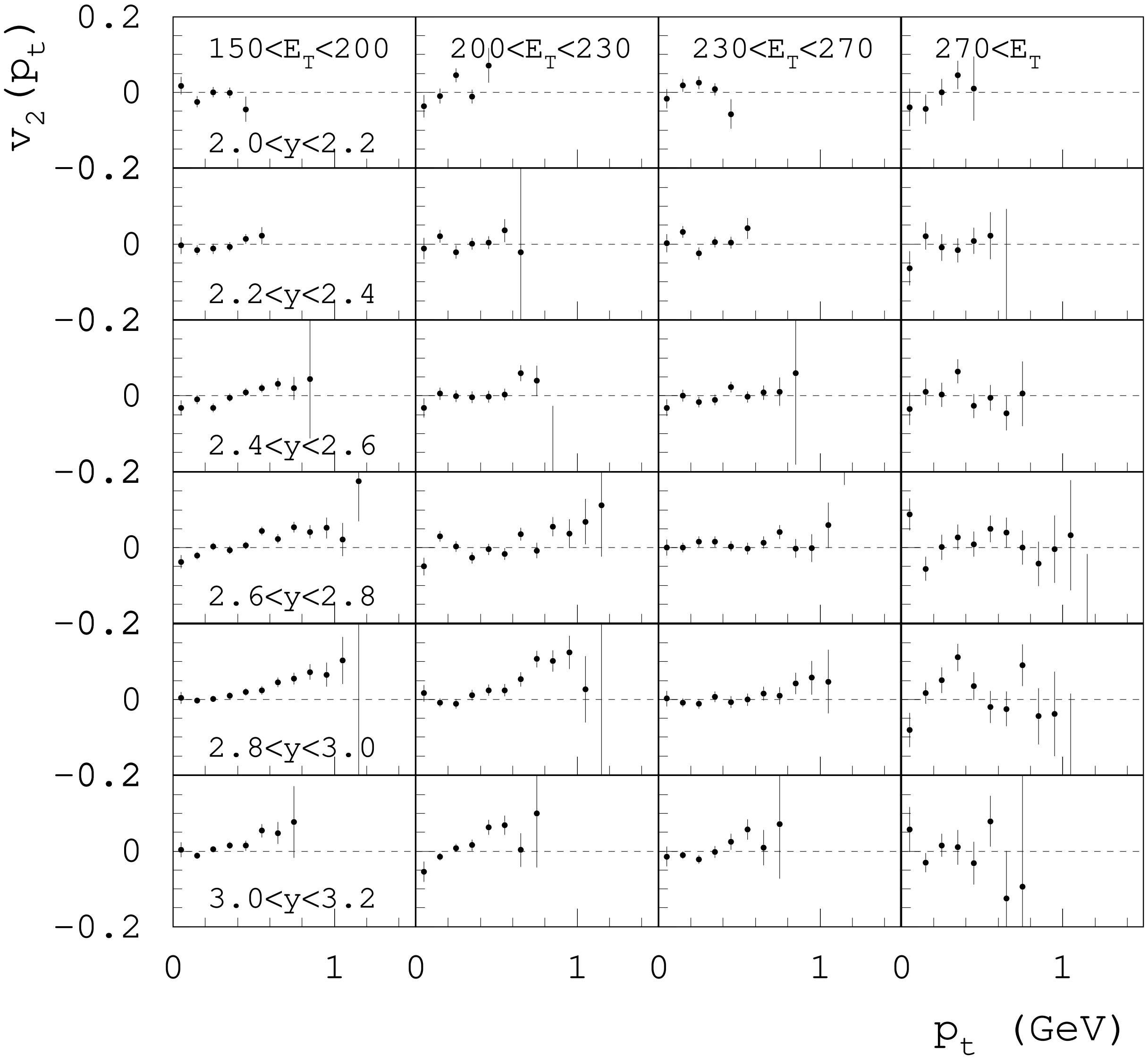

FIG. 5. The transverse momentum dependence of the second moment (v_2) of proton azimuthal distribution for different particle rapidities and centralities of the collision.

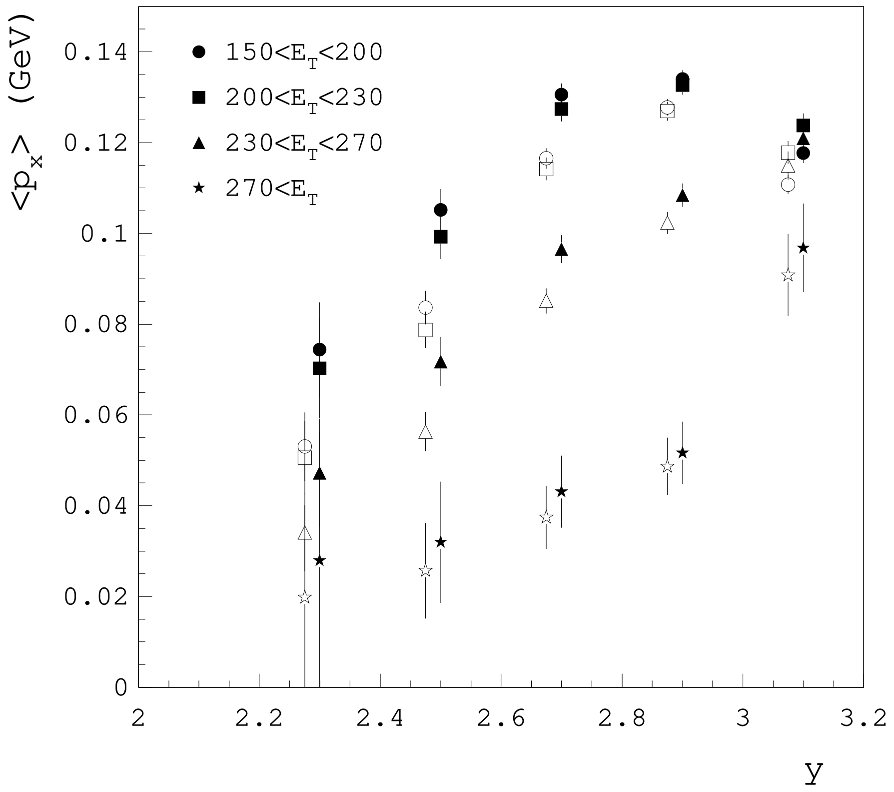

FIG. 6. Mean projection of the proton transverse momentum onto the reaction plane, $\langle p_x \rangle$, as a function of rapidity. Open points (shifted to the left by 0.05 for clarity) correspond to the fit by function (4).

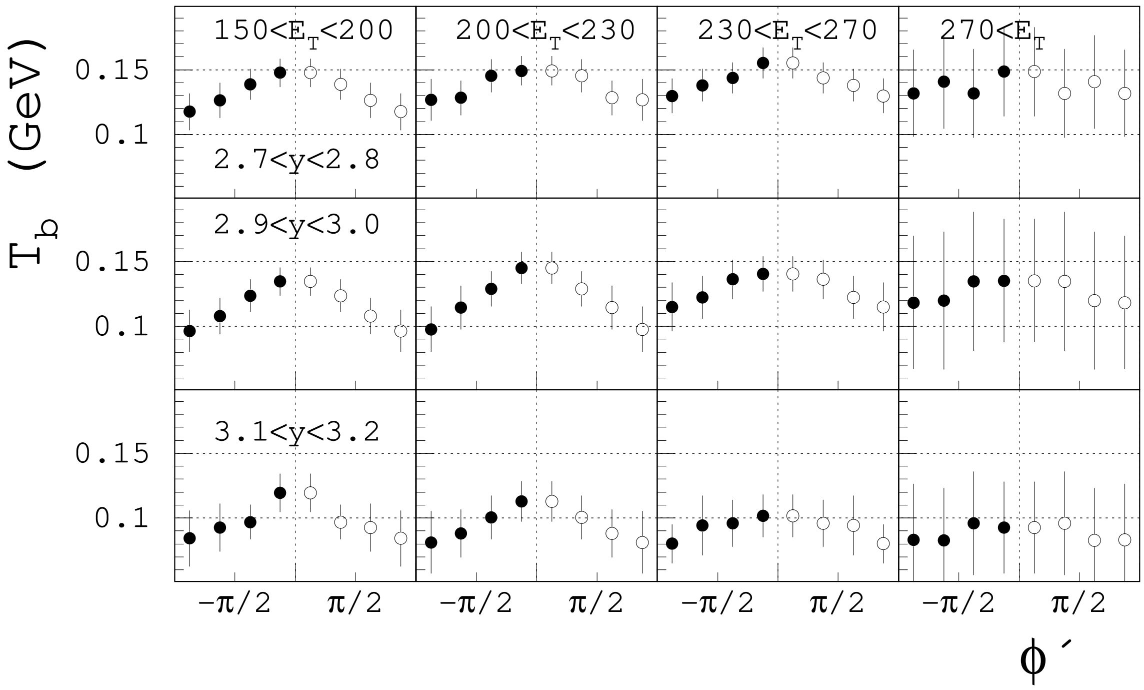

FIG. 7. The dependence of inverse (Boltzmann) slope (T_B) of proton distribution as a function of azimuthal angle. The open points are the reflection of filled ones around $\phi' = 0$.

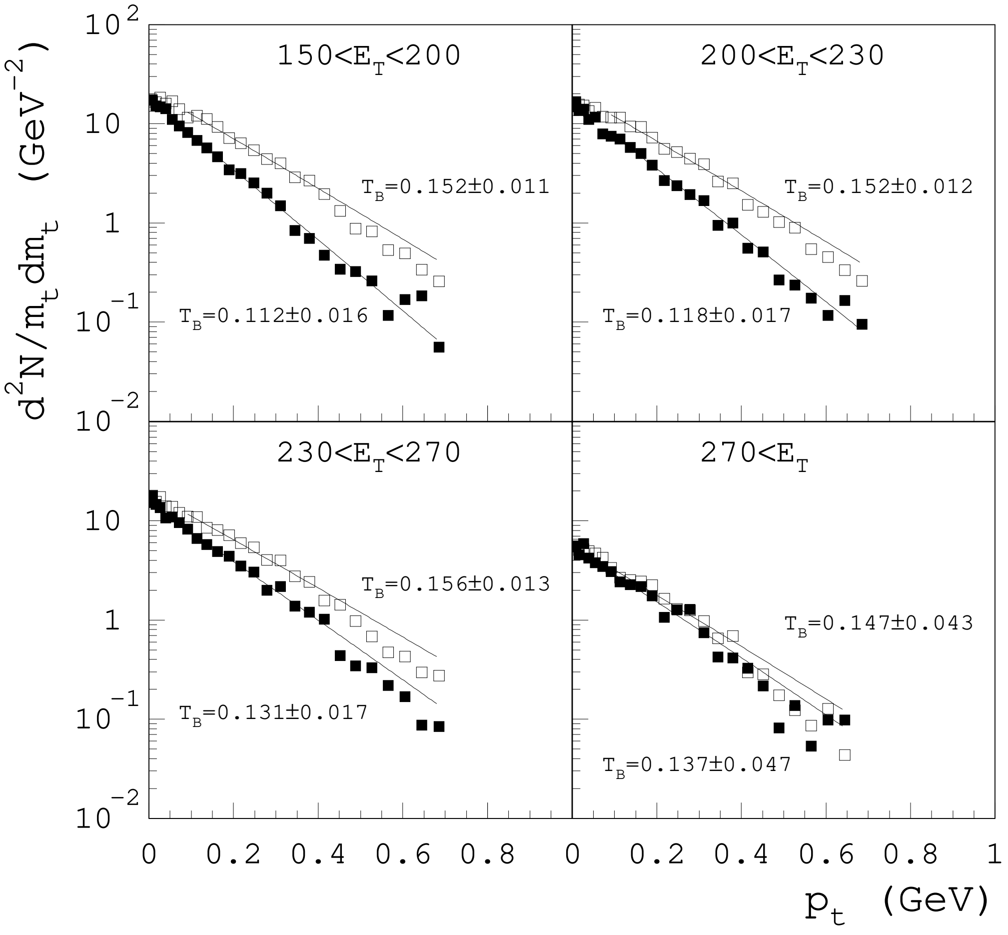

FIG. 8. The fit of proton m_t distributions in the rapidity interval $2.8 < y < 2.9$ by function (7). The effective slope values and centrality (PCal E_t) are shown in GeV. The open (filled) points correspond to $-\pi/4 < \phi' < \pi/4$ ($3\pi/4 < \phi' < 5\pi/4$).

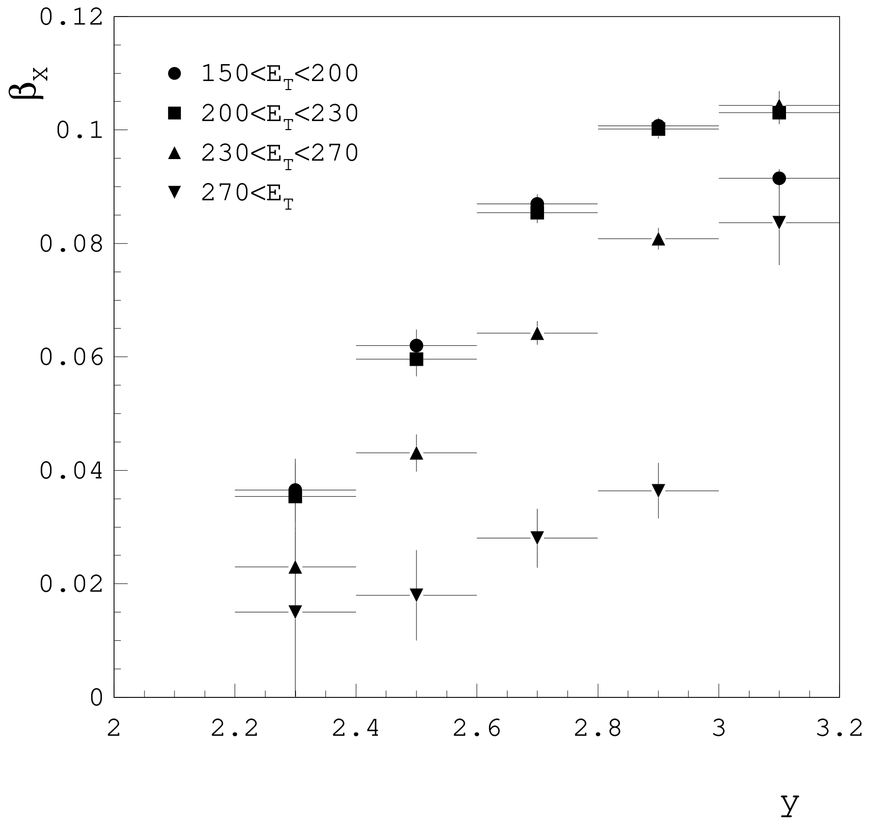

FIG. 9. Transverse velocity β_x of the thermal (proton) source for different rapidities and centralities of the collision (PCal E_T, in GeV).

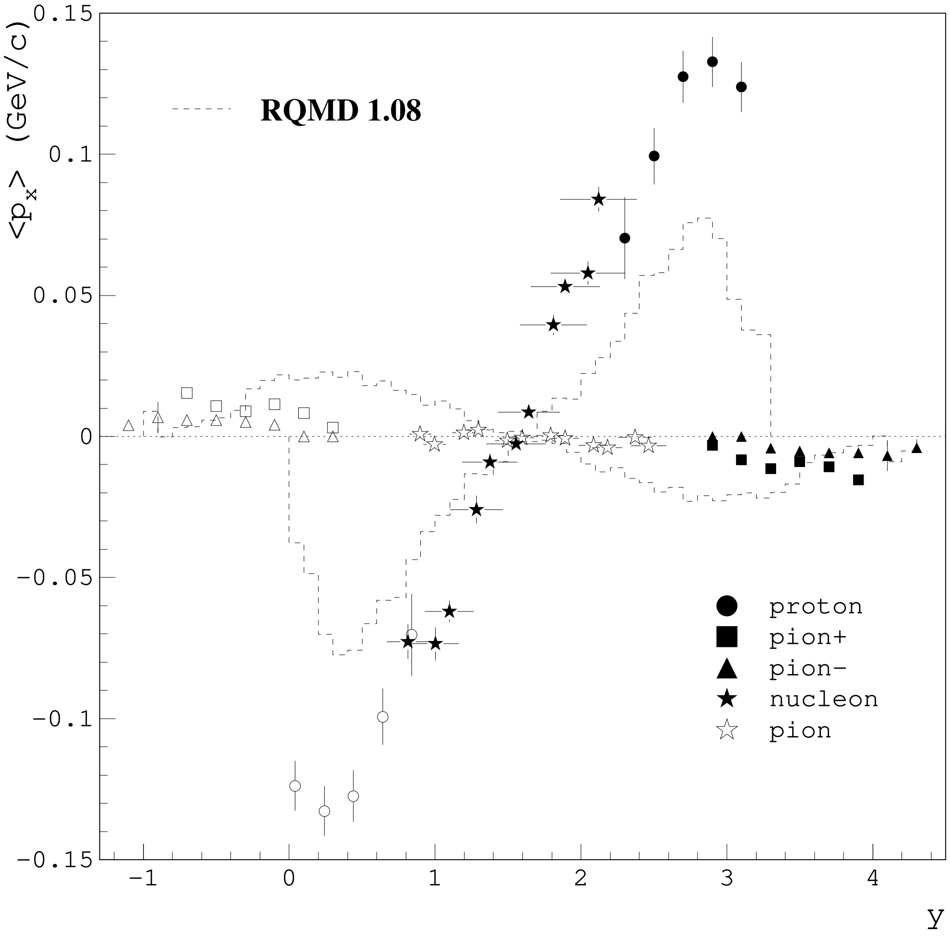

FIG. 10. Mean projection of the proton transverse momentum onto the reaction plane $\langle p_x \rangle$ as a function of rapidity. Open circles, triangles and squares are the reflection of filled ones. The results derived from measurements [2] are shown by stars. The histograms correspond to RQMD 1.08.